Algal Research 67 (2022) 102834

Contents lists available at ScienceDirect

Algal Research

journal homepage: www.elsevier.com/locate/algal

Green algae to green fuels: Syngas and hydrochar production from *Ulva lactuca* via sub-critical water gasification

Obie Farobie [a,b,*], Novi Syaftika [c], Imron Masfuri [c], Tyas Puspita Rini [c], Dovan P.A. Lanank Es [c], Asep Bayu [d], Apip Amrullah [e], Edy Hartulistiyoso [a,b], Navid R. Moheimani [f], Surachai Karnjanakom [g], Yukihiko Matsumura [h]

[a] *Department of Mechanical and Biosystem Engineering, Faculty of Agricultural Engineering and Technology, IPB University (Bogor Agricultural University), IPB Darmaga Campus, Bogor, West Java 16002, Indonesia*
[b] *Surfactant and Bioenergy Research Center (SBRC), IPB University (Bogor Agricultural University), Jl. Pajajaran No. 1, IPB Baranangsiang Campus, Bogor, West Java 16144, Indonesia*
[c] *Research Centre for Process Industry and Manufacturing Technology, National Research and Innovation Agency (BRIN), Kawasan PUSPITEK Serpong, Tangerang Selatan, Indonesia*
[d] *Research Center for Vaccine and Drugs, Research Organization for Health, National Research and Innovation Agency (BRIN), Jl. Raya Jakarta-Bogor KM 46 Cibinong, Bogor, West Java 16911, Indonesia*
[e] *Department of Mechanical Engineering, Lambung Mangkurat University, Banjarmasin, South Kalimantan, Indonesia*
[f] *Algae R&D Centre, Harry Butler Institute, Murdoch University, Murdoch, WA 6150, Australia*
[g] *Department of Chemistry, Faculty of Science, Rangsit University, Pathumthani 12000, Thailand*
[h] *Graduate School of Advanced Science and Engineering, Hiroshima University, 1-4-1 Kagamiyama, Higashi-Hiroshima 739-8527, Japan*

ARTICLE INFO

Keywords:
Algae
Chlorophyta
Hydrothermal
Hydrochar
Syngas

ABSTRACT

Biomass-derived energy is gaining more attention due to environmental issues and increasing energy demand. To ensure the sustainability of fossil energy substitution using biomass, diversification of sources, including marine organisms, is vital. Among various types of marine biomass discussed in the literature, the utilization of green algae *Ulva lactuca* for energy generation is still rare globally. Therefore, this study aims to investigate the potential of green fuel (syngas and hydrochar) production from *U. lactuca* (Chlorophyta) via sub-critical water gasification (SbWG). The experiments were conducted using a batch reactor at varying temperatures (300, 350, and 400 °C), reaction times (30, 60, and 90 min), and feedstock concentrations (1 and 5 wt%). The effect of temperature on gas composition was examined in detail. The results revealed that increasing temperature from 300 to 400 °C leads to an increase in the H_2 content significantly from 2.21 % to 8.09 % within 90 min. However, increasing feedstock concentration from 1 to 5 wt% reduces the H_2 fraction due to suppression of the steam reforming and water-gas shift reactions. Based on the ultimate analysis, the high severity of operating conditions leads to lower O/C and H/C atomic ratios owing to dehydration and decarboxylation reactions. It was confirmed by scanning electron microscope (SEM) analysis that more void structures existed in hydrochar than the algal feedstock. The SbWG process at varying temperatures and times can increase the energy contents of *U. lactuca* by over 47 %. Intriguingly, hydrochar obtained at 400 °C exhibited higher HHVs (i.e., 21.75–22.93 MJ kg^{-1}) than typical low-ranked coals, making hydrochar more potential to be used as solid fuels. Finally, a reaction model was deduced, and the decomposition of *U. lactuca* was confirmed to follow the Arrhenius behavior.

1. Introduction

Fossil fuel-derived energy is currently being used as the most viable transportation fuel worldwide [1]. Nevertheless, the prolonged and massive consumption of fossil fuels contributes to the declining energy source and causes severe environmental problems due to the emission of harmful pollutants, leading to global warming [2]. Needless to say, fossil-derived energy is deemed non-renewable and unstainable,

* Corresponding author at: Surfactant and Bioenergy Research Center (SBRC), IPB University (Bogor Agricultural University), Jl. Pajajaran No. 1, IPB Baranangsiang Campus, Bogor, West Java 16144, Indonesia.
E-mail address: obiefarobie@apps.ipb.ac.id (O. Farobie).

https://doi.org/10.1016/j.algal.2022.102834
Received 12 June 2022; Received in revised form 17 August 2022; Accepted 1 September 2022
Available online 6 September 2022

triggering enormous research efforts to find alternatively environmentally benign energy sources. This mitigation would also play a role in minimizing carbon emission and greenhouse gases (GHGs). One of the most promising and environmentally friendly alternative energy sources is biomass since it is globally available and considered utterly non-carbon benefits. It is because the released CO_2 to the environment when biomass is converted into energy is captured during biomass production through photosynthesis [3].

In biomass energy, diversification is vital to ensure sustainability, especially in addressing the land-use change issue to supply biomass [4]. Hence, marine resources, namely algal biomass (micro and macro) termed as the third generation of biomass, is expected to play an essential role in harvesting the energy since they have high organic content, rapid growth rate, and do not require arable land, and do not compete with agricultural crops over fresh water [5,6]. Microalgae with their high lipid content have been widely discussed in various research as raw materials for bioenergy production [7]. On the contrary, the studies on macroalgae, popularly known as seaweed as an energy resource, have not received much attention, although it is found abundantly [5,8].

Since severe problems in the aquatic environment by reducing the oxygen content in water, the excessive growth of macroalgae has been a worldwide concern for the freshwater and coastal regions [9,10]. Among several species of algae, sea lettuce, Sargassum, and water hyacinth have been reported to generate bloom causing eutrophication with the most common sea lettuce (*U. lactuca*) as a green seaweed [11–14]. To address this issue, the valorization of *U. lactuca* to alternative energy would enable us to answer the shortcomings caused by the marine pollution problem as well as environmental pollutions due to fossil fuel combustion.

Numerous biological and thermochemical techniques are developed to produce renewable energy from biomass. A biological approach including anaerobic digestion and alcoholic fermentation to convert biomass into energy is considered less energy-intensive than the thermochemical route [6]. Nevertheless, the biological conversion has significant drawbacks of long processing time, low tolerance to heavy metals, the stringent requirement of temperature and pH, and low conversion technology [15,16]. Hence, thermochemical methods, such as torrefaction, combustion, pyrolysis, gasification, hydrothermal process, are considered as suitable techniques for biomass conversion into energy due to their efficiency and simplicity, and well-understood operation [17–19]. However, one of the challenges in the valorization of macroalgae is the natural water content and the associated need for drying the biomass prior to thermal conversion. Hence, one of the most promising techniques to convert wet biomass is hydrothermal processing, including hydrothermal liquefaction, carbonization, and gasification owing to the reduction of energy-intensive drying steps, resulting in saving cost and energy [20].

Very few studies have reported biofuel production potential from *Ulva* sp. using hydrothermal processes, including hydrothermal carbonization and hydrothermal liquefaction [10,21–24]. Yan et al. [21] have reported the hydrothermal liquefaction of *U. prolifera* in the presence of a base catalyst at varying temperatures (270–310 °C) and reaction time (10–30 min). They found that the bio-crude oil as much as 12.0 wt% and 26.7 wt% was achieved at non-catalytic and KOH-catalyzed liquefaction, respectively. Furthermore, Ma et al. [23] showed that the hydrothermal liquefaction of *U. prolifera* over a zeolites-based catalyst at 280 °C increased the bio-crude oil yield by over 44 %. Xu et al. [22] also conducted the catalytic behavior of hydrothermal liquefaction of *U. prolifera* at different temperatures (260–300 °C) and time (15–45 min). Their result revealed that the highest bio-crude oil yield of 35.1 wt% was obtained over the metal MgO catalyst. Moreover, Steinbruch et al. [24] investigated the production of monosaccharides, polyhydroxyalkanoates (PHA), and hydrochar from the hydrothermal processing of *Ulva* sp. Further, Shrestha et al. [10] reported the hydrochar production through hydrothermal carbonization of *U. lactuca* at operating temperature and time of 150–220 °C and 30–120 min, respectively. They found that the HHV of hydrochar obtained from hydrothermal carbonization of *U. lactuca* is in the range of 13.4–20.2 MJ kg^{-1}.

Previous studies give insights that bio-crude oil and hydrochar can be produced from *Ulva* sp. through hydrothermal liquefaction and hydrothermal carbonization. However, the previous works focused on liquid (bio-crude oil) and solid (hydrochar) products. It should be noted that *U. prolifera* is the most used green algae for biofuel production in the previous works. The valorization of *U. lactuca* for biofuels is still rarely investigated. Furthermore, there are no reports on the simultaneous production of syngas and hydrochar from *U. lactuca* via sub-critical water gasification (SbWG) to the best of our knowledge. The SbWG process effectively dissolves and converts biomass into the desired product by modifying its operating parameters, typically at a temperature range of 150 to 374 °C under sufficient pressure to keep water in the liquid state [25–27]. Bio-syngas is fuel gas derived from biomass consisting of a mixture of hydrogen (H_2), carbon monoxide (CO), and very often some carbon dioxide (CO_2). Hydrogen is not just attractive as green energy but also an essential gas for various chemical industries [6]. On the other hand, hydrochar is a carbon-rich solid with characteristics that allow it to be applied for various purposes such as energy storage and solid-combustion fuel [28]. To design the efficient and effective use of *U. lactuca* for syngas and hydrochar production using the SbWG method, comprehensive studies are necessary. Thus, this work discusses the effect of temperature, holding time, and feedstock concentration on product distribution, kinetic model, and characteristics of syngas and hydrochar products from *U. lactuca* under sub-critical water conditions in detail.

2. Materials and methods

2.1. Feedstock preparation and analysis

The feedstock of *U. lactuca* was collected from Ekas beach, Lombok Island, Indonesia. The fresh macroalgal feedstock was initially cleaned with tap water to remove the sand and debris, then rinsed with distilled water. Afterward, the macroalgal sample was dried using an oven at 50 °C for 3 h. The dried sample was then ground using a coffee bean grinder and subsequently sieved to achieve a uniform particle size of 0.25 mm. Please note that the drying process of the sample in this study was conducted to ensure the precise concentration of feedstock. For the implementation stage of this technology, the drying process can be eliminated by adjusting the water content of the feedstock.

Proximate analysis of feedstock was conducted using a thermogravimetric analyzer TGA 4000 (Perkin Elmer, United States) following the ASTM E1131-08. The moisture content was determined from the weight loss of the sample after being heated at 110 °C in an inert atmosphere with pure N_2. The volatile matter was measured from the weight loss of the sample at 900 °C. Meanwhile, the ash content was determined by switching the N_2 to air and keeping isothermally at 900 °C for 45 min. The fixed carbon (FC) value was determined using the following formula:

$$\text{FC (wt\%)} = 100\text{–(volatile matter wt\%} + \text{moisture wt\%} + \text{ash wt\%)}$$

The higher heating value (HHV) of the feedstock was calculated using a bomb calorimeter (Parr 6200 Isoperibol) according to ASTM D 5865–04. Furthermore, the ultimate analysis of carbon (C), hydrogen (H), and nitrogen (N) was determined using a CHN628 analyzer (Leco). Meanwhile, the sulfur (S) analysis was carried out using the CHN632 analyzer (Leco). The oxygen (O) content was calculated using a formula as follows:

$$\text{Oxygen (\%)} = 100\text{–(\%C} + \text{\%H} + \text{\%N} + \text{\%S)}$$

All the analysis was conducted at least three times to obtain reproducible data. The proximate and ultimate analysis of *Ulva* sp. is

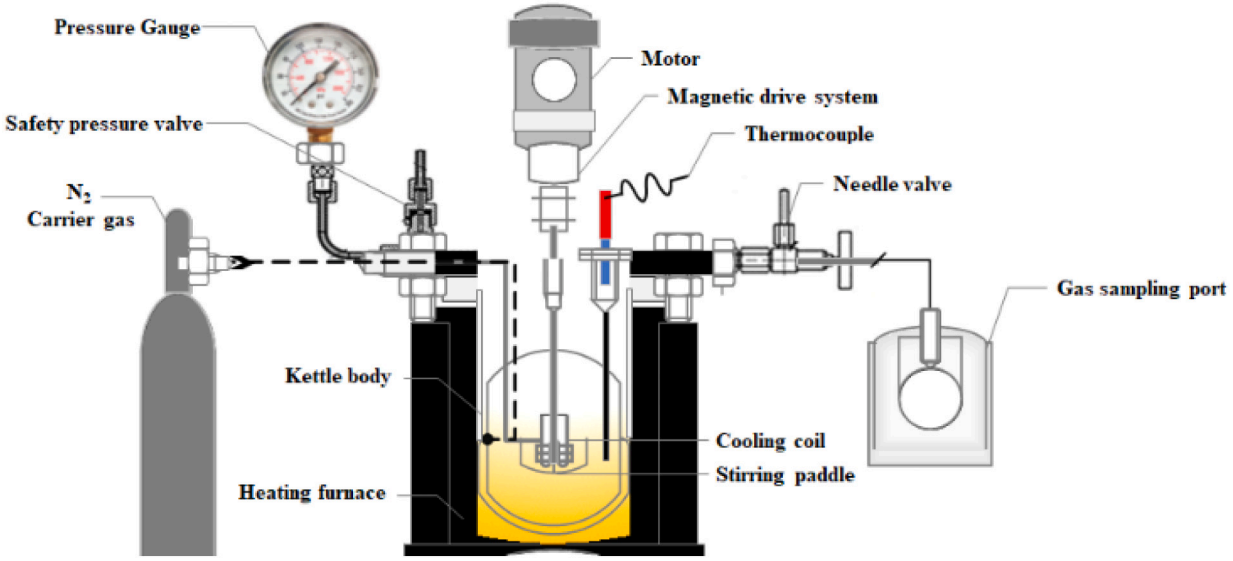

Fig. 1. A schematical diagram of the experimental apparatus.

summarized in Table S1.

2.2. Sub-critical water gasification of U. lactuca

The sub-critical water gasification of the *Ulva* sp. was carried out using a 500 mL Parr reactor (Model 4575, Parr Instrument Co.) with a batch mode schematically illustrated in Fig. 1. The temperature profile of this reactor for the operating condition of SbWG of *U. lactuca* is provided in Fig. S1. The reactor was equipped with a block element electric heater, a removable vessel, a magnetic drive agitator, a temperature controller Autronics TZN4s, and a data logger. The reactor was designed for an operating temperature of 500 °C and a pressure of 34.5 MPa.

The desired amount of dried sample (1 and 5 wt%) was added to the reactor. Afterward, the reactor was sealed and purged with pure N_2 gas to remove air. The SbWG process was conducted at several temperatures (300, 350, and 400 °C) and holding times (30, 60, and 90 min). The reactor's pressure was set at 8 MPa under a nitrogen atmosphere, and the suspension was stirred at 100 rpm. The reactor was cooled rapidly using a cooling water chamber after completing the SbWG reaction. After that, the gas product was carefully collected, and the yield was calculated based on the reactor pressure using the ideal gas equation. In the meantime, the reaction mixture was then filtered by vacuum filtration, and the solid residue (hydrochar) was dried in the oven at 60 °C for 24 h. The product yields were calculated by gravimetry and based on the initial mass feedstock. All experiments were conducted in duplicate.

2.3. Characterization of syngas and bio-char

The gaseous products from SbWG of *Ulva* sp. were analyzed using two gas chromatographs (GC Shimadzu 8A, Japan). One is equipped with a thermal conductivity detector (TCD), a Shincarbon ST 50/80 mesh column, and He as the carrier gas to analyze H_2 CH_4, CO_2, and CO. Meanwhile, another GC is equipped with a flame ionization detector (FID), a Porapak Q column, and He as the carrier gas to analyze C_2H_4 and C_2H_6. The temperature inside the column was isothermally set at 50 °C. Meanwhile, the injector and detector temperatures were both set at 100 °C.

The elemental composition of hydrochar was characterized using an elemental (C, H, N, S) analyzer with the same methods used for the feedstock. Meanwhile, Hydrochar was analyzed using an infrared spectrometer Spectrum Two Universal ATR–FT-IR (Perkin Elmer, United States) at 400–4000 cm^{-1} wavelength to evaluate the appearance of functional groups in the hydrochar. The hydrochar morphology was also examined by Scanning Electron Microscope (Hitachi, SU 3500).

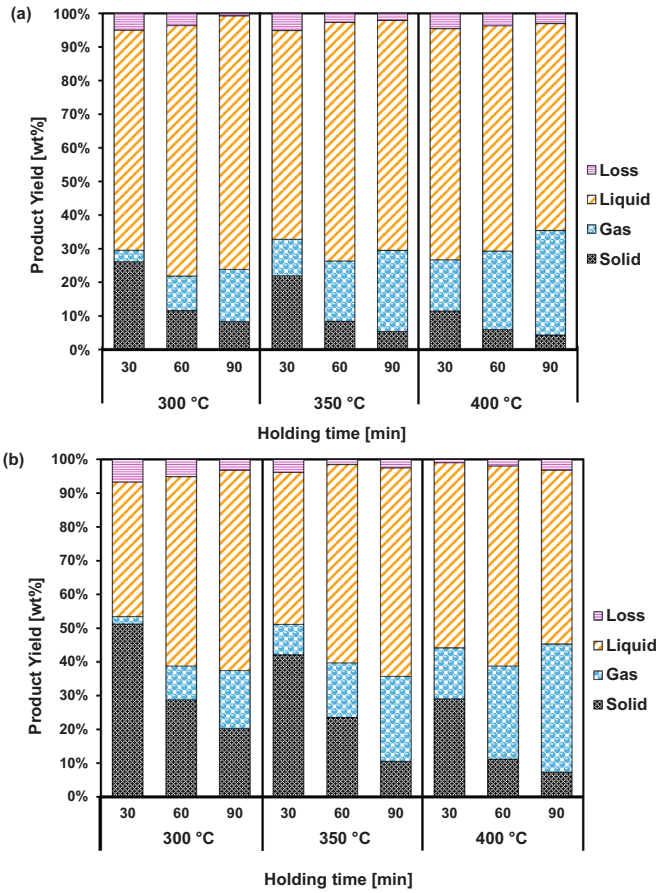

Fig. 2. Effect of temperature and time on product distributions of *U. lactuca* via sub-critical water gasification at feedstock concentration (a) 1 wt% and (b) 5 wt%.

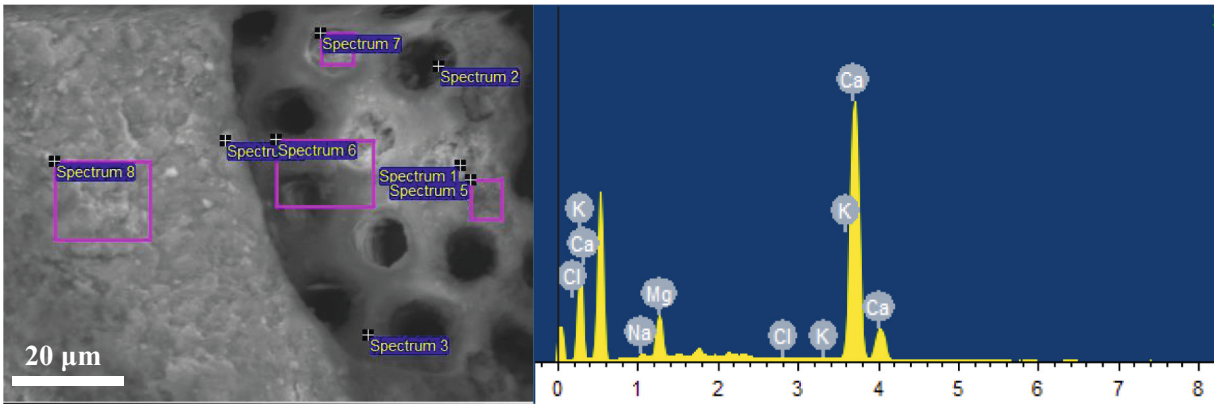

Fig. 3. Scanning electron microscope–energy dispersive X-ray (SEM–EDX) analysis of the dried biomass of *U. lactuca*.

3. Results and discussion

3.1. Effect of temperature on product distribution

The effect of temperature on the product distribution of SbWG of *U. lactuca* is presented in Fig. 2. At a dilute feedstock concentration (1 wt %), the gas yields significantly increased with temperature and reaction time. The gas yields increased from 3.42 % to 15.20 % when the reactions occurred from 300 to 400 °C at 30 min. The yields were higher when the reactions were performed at 60 min, increasing from 10.24 % to 23.39 %. Meanwhile, when the reaction time was further prolonged to 90 min, a substantial increase in gas yield was observed from 15.60 % to 31.10 %, increasing operating temperature from 300 °C to 400 °C. It can be explained due to the more significant breakdown of low molecular weight compounds in the liquid phase into non-condensable gas occurring at higher temperatures and longer reaction times.

The linear trend of temperature and gas yield has been linked to the rapidly changing water properties with temperature. In the vicinity of a critical point of water (374 °C), the physical properties of water, i.e., viscosity, density, and dielectric constant, change dramatically. Hence, it enables water to act like a non-polar solvent, resulting in miscibility with gases. The higher amount of gas produced at high temperature during the hydrothermal process of biomass has been observed by other researchers [21,29,30].

In contrast with the gas trend, the yield of hydrochar decreased with reaction temperature and time. This result should be attributed to; (1) more significant primary decomposition of macroalgal biomass (carbohydrates, lipids, and proteins) at higher temperatures and longer reaction times to generate liquid and gas products [31], and (2) secondary decomposition of hydrochar during the carbonization process under severe conditions [32]. At 400 °C, the hydrochar yield dramatically decreased, which may be due to the degradation of macromolecules in macroalgae into liquid and gaseous phase products instead of retaining in the solid phase.

It is also clearly noticeable that the liquid yield increased with prolonged reaction time from 30 to 60 min, but it then slightly decreased once the reaction time was prolonged further to 90 min at 300 and 350 °C. The increase in liquid yield when prolonging the reaction time from 30 to 60 min could be attributed to an increase in the primary decomposition reactions of the algal biomass, such as thermal cracking and dehydration. Meanwhile, the decrease in liquid yield as the reaction time was further prolonged to 90 min could be due to the secondary decomposition of the products, enhancing gas products such as CH_4, H_2, and CO_2. At 400 °C, the liquid yield relatively decreased with a longer reaction time. It is supported by the fact that the gas yield observed at 400 °C was significantly higher than those at 300 °C and 350 °C. The increasing temperature should improve the decomposition of organic compounds, especially the possible in situ catalytic by the alkali as well as alkaline earth metal contained in *U. lactuca*. In the previous experiments, macroalgae have been reported to contain a high amount of alkali and alkaline earth metals such as Ca and Na. These metals were responsible for enhancing carbonaceous materials degradation and char reforming during gasification to generate gas products [33–35]. In our study, the high ash content of *U. lactuca* was found as presented in the proximate and ultimate analysis of feedstock (see Table S1).

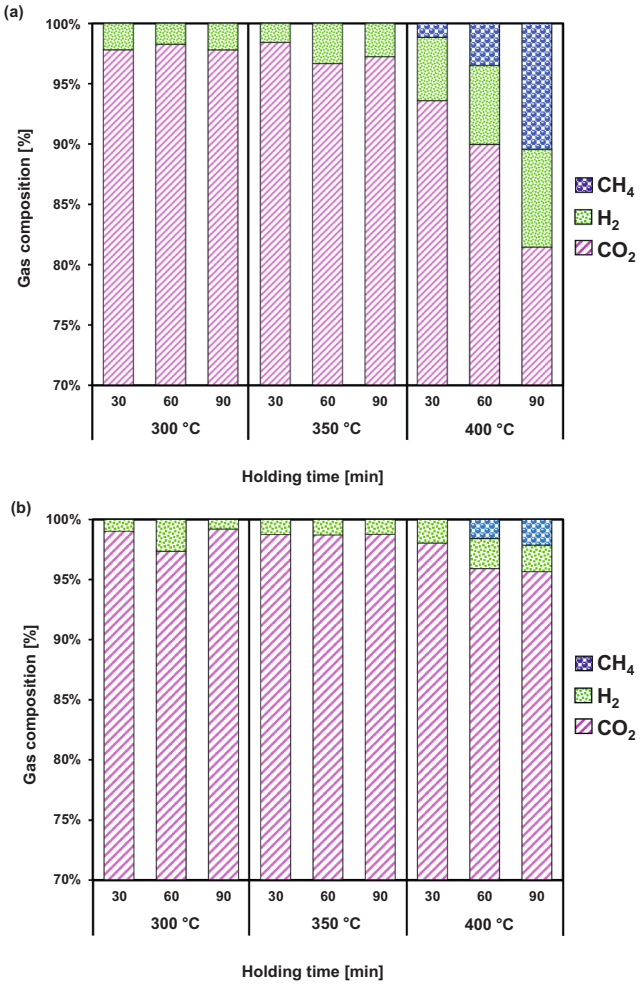

Fig. 4. Effect of temperature and time on gas composition after sub-critical water gasification of *U. lactuca* at feedstock concentration of (a) 1 wt% and (b) 5 wt%.

Table 1
Ultimate and heating values of hydrochar from sub-critical water gasification of *U. lactuca*.

Feedstock loading	Temperature [°C]	Holding time [min]	Ultimate analysis (wt%)					HHV (MJ kg^{-1})
			% C	% H	% N	% S	% O	
Feedstock (*U. lactuca*)			39.10 ± 0.05	6.20 ± 0.05	4.46 ± 0.02	7.28 ± 0.03	42.96 ± 0.05	12.04 ± 0.03
1 wt%	300	30	45.57 ± 0.50	4.74 ± 0.08	1.88 ± 0.02	6.45 ± 0.06	41.35 ± 0.54	19.03 ± 0.02
		60	47.19 ± 0.07	4.65 ± 0.04	2.00 ± 0.02	6.58 ± 0.05	39.59 ± 0.03	20.20 ± 0.02
		90	47.63 ± 0.21	4.55 ± 0.04	2.24 ± 0.01	6.81 ± 0.04	38.97 ± 0.29	20.31 ± 0.03
	350	30	48.06 ± 0.17	4.63 ± 0.09	1.77 ± 0.06	6.74 ± 0.04	38.80 ± 0.37	19.29 ± 0.02
		60	49.07 ± 0.07	4.19 ± 0.05	2.07 ± 0.05	7.15 ± 0.04	37.52 ± 0.21	20.41 ± 0.02
		90	49.12 ± 0.05	3.81 ± 0.05	2.11 ± 0.03	6.60 ± 0.13	38.36 ± 0.06	21.32 ± 0.04
	400	30	51.46 ± 0.11	3.71 ± 0.06	2.15 ± 0.09	7.85 ± 0.06	34.83 ± 0.21	21.75 ± 0.03
		60	51.50 ± 0.06	3.64 ± 0.06	2.28 ± 0.01	8.17 ± 0.06	34.41 ± 0.16	22.09 ± 0.04
		90	53.15 ± 0.11	3.15 ± 0.10	2.17 ± 0.04	7.56 ± 0.04	33.98 ± 0.08	22.32 ± 0.03
5 wt%	300	30	51.87 ± 0.06	3.95 ± 0.02	1.96 ± 0.04	6.85 ± 0.07	35.37 ± 0.19	19.61 ± 0.04
		60	52.51 ± 0.73	3.31 ± 0.08	1.96 ± 0.01	6.92 ± 0.01	35.30 ± 0.82	20.85 ± 0.04
		90	53.19 ± 0.10	2.89 ± 0.04	1.98 ± 0.01	8.94 ± 0.04	33.00 ± 0.09	21.30 ± 0.02
	350	30	54.67 ± 0.16	3.19 ± 0.04	2.15 ± 0.04	7.43 ± 0.07	32.56 ± 0.17	19.69 ± 0.02
		60	54.87 ± 0.11	3.08 ± 0.05	2.17 ± 0.02	7.29 ± 0.04	32.60 ± 0.12	21.11 ± 0.02
		90	55.17 ± 0.84	2.8 ± 0.05	2.29 ± 0.04	7.98 ± 0.02	31.77 ± 0.78	21.32 ± 0.04
	400	30	56.70 ± 0.09	3.11 ± 0.06	2.40 ± 0.03	7.70 ± 0.05	30.09 ± 0.11	21.75 ± 0.03
		60	56.81 ± 0.04	3.06 ± 0.04	2.14 ± 0.01	10.20 ± 0.05	27.69 ± 0.04	22.84 ± 0.02
		90	56.94 ± 0.06	3.01 ± 0.08	2.31 ± 0.03	9.04 ± 0.04	28.70 ± 0.03	22.93 ± 0.02

Furthermore, it was supported by the SEM-EDX analysis, which exhibited the high contents of alkali and alkaline earth metal species, especially Ca (90.13 wt%), Mg (8.51 wt%), and Na (1.05 wt%) (Fig. 3).

At the feedstock concentration of 5 wt%, the product distribution trend is similar to 1 wt%. However, the hydrochar yield was significantly higher than that obtained at 1 wt%. It could be because the increased feedstock concentration from 1 to 5 wt% could reduce the possibility of thermal decomposition of macroalgal biomass, resulting in high hydrochar yield. This result is following the former research of Arun et al. [36], who reported that a high concentration of feedstock during the hydrothermal process leads to solid residue formation due to incomplete degradation. Another possibility is due to char formation, whose reaction is enhanced for higher concentration, and thus the liquid product is consumed more for char production and thus gasification is suppressed.

3.2. Effect of temperature on gas composition

GC/MS analysis was conducted to determine the composition of bio-oil where the peak area percentage of the detected compounds is related to the response factor.

The effect of temperature on gas composition is shown in Fig. 4. As can be seen, the gaseous products from SbWG of *U. lactuca* mainly consist of CO_2 and low content of CH_4 and H_2. At a feedstock concentration of 1 wt%, the high reaction temperature and long reaction time had a positive trend on H_2 production. The H_2 content increased 2.4-fold when the reaction temperature was increased from 300 to 400 °C at 30 min. The increase of H_2 production was observed when the reaction time was extended to 60 min, yielding H_2 production to increase 3.8-time. However, prolonging a reaction at 90 min did not significantly enhance the H_2 production, i.e., 3.7-folds, compared with that at 60 min. Even though the maximum H_2 yield increased about 2.21 to 8.09 % as the operating temperature increased from 300 to 400 °C. It should be noted that the significant effect of operating conditions (temperature and time) on the yield of H_2 during biomass gasification was also mentioned in the literatures [37–39].

The higher H_2 fraction with increasing the operating temperature and time might be due to the thermal decomposition of intermediates, as proposed by Acelas et al. [40]. It could also be attributed to the nature of the biomass gasification process, which undergoes the steam reforming reaction and water-gas shift reaction as depicted in Eqs. (1) and (2), respectively. Since the steam reforming reaction is endothermic, it is enhanced with high temperature, enabling to increase in the H_2 fraction [41]. Water-gas shift reaction is also promoted at the higher temperature, increasing H_2 content [42]. Apart from that, H_2 is mainly generated via free-radical reaction. Below the critical point of water, the ionic reaction is more dominant, and the aqueous phase is favourable to undergo the free-radical gas reaction above the critical point of water [43].

$$CHxOy + (1–y)\ H2O \rightarrow CO + (1–y+x/2)\ H2 \quad (1)$$

$$CO + H2O \leftrightarrow CO2 + H2 \quad (2)$$

It is worth noting that no CH_4 is observed at low temperatures of 300 and 350 °C, but CH_4 production was enhanced in supercritical conditions (400 °C). It could be attributed to the methanation reaction (see Eq. (3)) being promoted when the H_2 is sufficient in the system. It is plausible to occur because the high H_2 fraction was found at 400 °C, leading to the CH_4 production at this state.

$$CO + 3H2 \leftrightarrow CH4 + H2O \quad (3)$$

At feedstock concentration of 5 wt%, the trend of gas composition was utterly different from that at 1 wt%. As clearly observed in Fig. 4, the H_2 fraction was significantly lower than obtained at 1 wt%. It can be explained that at low feedstock concentration (1 wt%), the surplus water can shift the steam reforming and water-gas shift reaction forward, leading to increase H_2 yield [6,39]. On the other hand, at high feedstock concentration (5 wt%), water deficiency can reduce the steam reforming and water-gas shift reactions, potentially reducing H_2 yields. The results of this finding follow the previous studies [44,45]. Graz et al. [44] reported that when the *Ulva* sp. concentration was increased from 7 to 16.4 wt%, H_2 yields sharply decreased from 2.7 to 1.8 mol/kg. Furthermore, Norouzi et al. [45] explored the effect of feedstock concentration on SCWG of *E. intestinalis* macroalgae. They observed that when the concentration of *E. intestinalis* was increased from 1 wt% to 2 wt%, the H_2 yield reduced significantly from 4.07 to 2.55 mol H_2/kg algae. Overall, the results emphasized that increased macroalgal loading could reduce the H_2 yields due to the suppressed steam reforming and water-gas shift reactions.

In general, the overall biomass gasification reaction is performed following Eq. (4), where *a* represents the molar ratio of H/C and *b* corresponds to the molar ratio of O/C. Based on this reaction, the main products from sub- and supercritical water gasification of biomass are CO_2 and H_2. The finding of this study is in accordance with this overall reaction. The low amount of CH_4 was observed in this study from the intermediate reaction of methanation, as depicted above. It is worthwhile to mention that no CO was found in this study, which might be because CO was consumed through the water-gas shift reaction (Eq. (2))

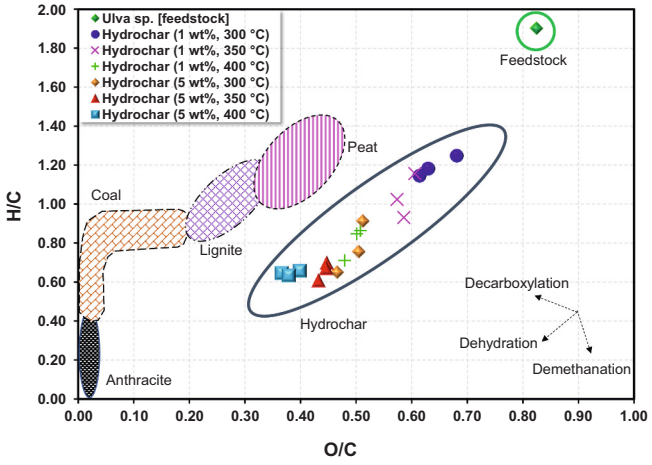

Fig. 5. Van Krevelen diagram of the hydrochar from sub-critical water gasification of *U. lactuca*.

and methanation reaction (Eq. (3)).

$$CHaOb + (2–b)\ H2O \rightarrow CO2 + (2–b+a/2)\ H2 \quad (4)$$

3.3. Characteristics of hydrochar

Hydrochar obtained from SbWG of *U. lactuca* was analyzed in terms of ultimate and heating values, the functional group using FTIR, and morphology using SEM to better understand its behavior during the gasification process.

3.3.1. Ultimate and heating values

The results of ultimate analysis and heating values measurement of hydrochar derived from SbWG of *Ulva* sp. at 300, 350, and 400 °C are presented in Table 1. Please note that feedstock's elemental composition and heating values are also presented for comparison purposes. The SbWG process altered the elemental composition of the hydrochar at varying temperatures and times. In general, hydrochar has high C content (45.57–56.94 %), low H content (3.01–4.74 %), and moderate O content (27.69–41.35 %). Compared with the C content of the macroalgal feedstock (39.10 %), the C content of hydrochar increased with increasing temperature, time, and feedstock concentration, confirming an increase in their energy density. The highest C content (56.94 %) was achieved from the SbWG reaction at 400 °C, 90 min, and 5 wt% feedstock concentration, whereas the lowest C content (45.57 %) was obtained at 300 °C, 30 min, and 1 wt% feedstock concentration. The increasing C content of hydrochar with increasing temperature and time has been linked to the condensation and aromatization taking place in subcritical water [10,29,31]. On the other hand, the hydrochar's H and O contents decreased with temperature and time due to demethanation, dehydration, and decarboxylation reactions, which were enhanced with the increasing temperature. [46] The low hydrogen content of hydrochar was also possibly due to the aromatization and formation of hydrogen gas (H_2). It should be noted that the nitrogen content of hydrochar derived from SbWG of macroalgae decreased with increasing temperatures. It may be because nitrogen is released in the gas phase when the temperature increases.

Furthermore, the hydrochar produced from the SbWG process contained higher energy (19.03–22.93 MJ kg^{-1}) than *U. lactuca* (12.04 MJ kg^{-1}). The lowest HHV (19.03 MJ kg^{-1}) was obtained from the reaction at 300 °C, 30 min, and 1 wt% feedstock concentration, whereas the highest HHV (22.93 MJ kg^{-1}) was produced from the reaction at 400 °C, 90 min, and 5 wt% feedstock concentration. It is intriguing to mention that the HHVs of hydrochar obtained from the reaction at 400 °C and 5 wt% feedstock concentration (21.75–22.93 MJ kg^{-1}) are comparable

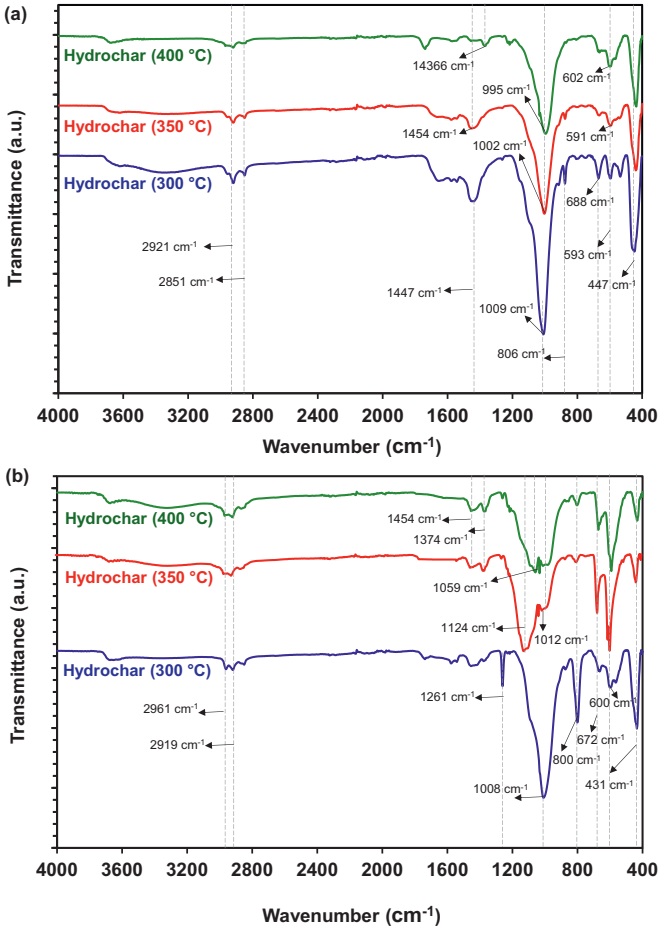

Fig. 6. FTIR spectra of the hydrochar from sub-critical water gasification of *U. lactuca* at feedstock concentration of (a) 1 wt% and (b) 5 wt%.

with those of the low-ranked coals. According to Luo and Tao [47], low-ranked coals typically have the HHV of 15 MJ kg^{-1}, but the values vary in the range of 12–25 MJ kg^{-1}. The high carbon content and calorific values of hydrochar indicated that macroalgal hydrochar could be used as solid fuel.

Besides HHV, the O/C and H/C atomic ratios are also considered in this study to investigate the characteristics of biomass for energy application. Fig. 5 shows the interpretation of O/C and H/C atomic ratios from the SbWG of *U. lactuca* by the van Krevelen diagram. Notably, hydrochar has lower O/C and H/C atomic ratios than the feedstock. Furthermore, high temperature and long reaction time lead to lower O/C and H/C atomic ratios of the solid product. The feedstock's O/C and H/C atomic ratios are 0.82 and 1.90, respectively. Meanwhile, the hydrochar obtained from the reaction of 1 wt% of feedstock had the O/C atomic ratios of 0.61–0.68; 0.59–0.61; and 0.48–0.51, respectively. The results confirmed that decarboxylation and cleavage of ether and ester bonds of organic components of the feedstock through hydrolysis were enhanced with the high temperature. The H/C atomic ratios of hydrochar also sharply decreased in the range of 1.15–1.25; 0.93–1.16; and 0.71–0.86 as an increase in temperatures of 300, 350, and 400 °C, respectively, indicating that the removal of hydroxyl groups through dehydration occurred throughout the subcritical water process. It is worthwhile noting that the O/C and H/C atomic ratios at feedstock concentration of 5 wt% were relatively lower than those obtained from the reaction of 1 wt% feedstock. One plausible reason is the carbonization reaction that leads to high C content remaining in hydrochar. In summary, the low O/C and H/C atomic ratios of hydrochar indicated its high carbon stability and high aromatic derivatives, as presumed by

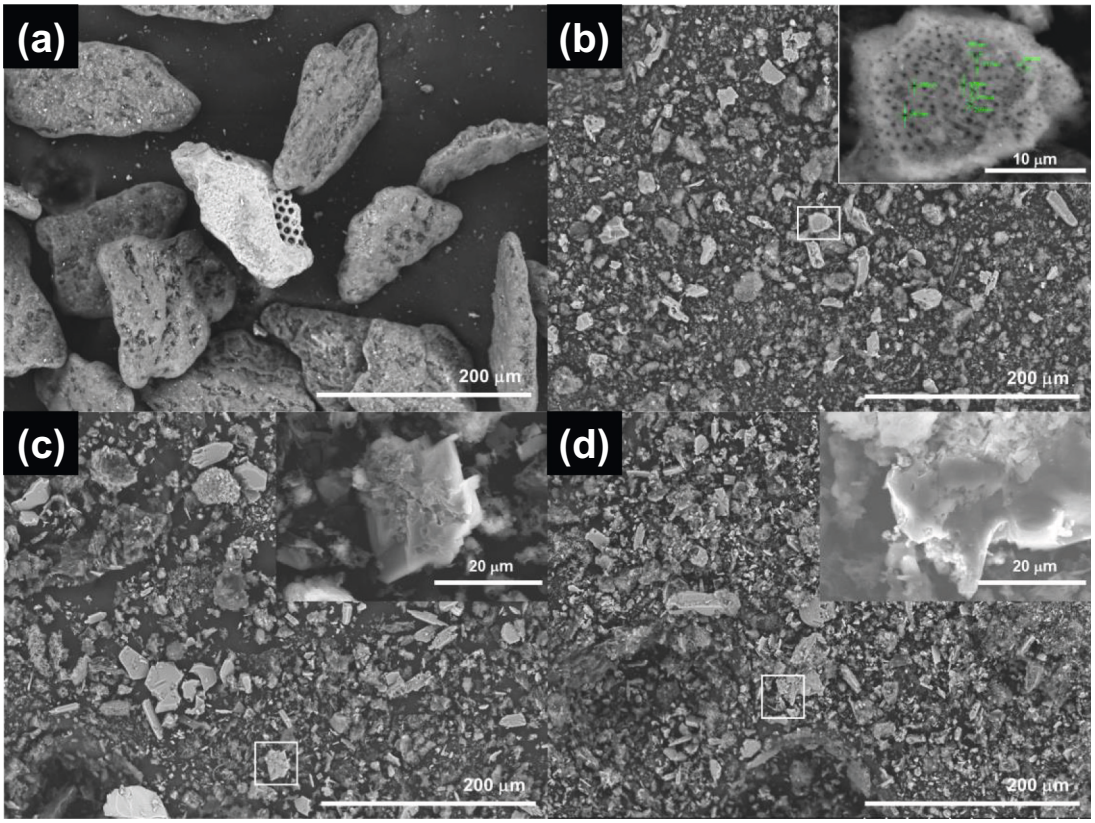

Fig. 7. SEM images of (a) untreated *U. lactuca* and hydrochar at (b) 300 °C, (c) 350 °C, and (d) 400 °C.

Gasco et al. [48].

3.3.2. FTIR spectra

The typical FTIR spectra of hydrochar produced through SbWG of *U. lactuca* are shown in Fig. 6. Meanwhile, the details of the typical band assignment of hydrochar at different temperatures are presented in Table S2. The FTIR spectra of hydrochar exhibited no broadband observed at 3000–3500 cm^{-1} representing the O—H stretching vibration, confirming that the SbWG process promotes the dehydration reaction.

At 1 wt% feedstock concentration, the bands between 2851 and 2921 cm^{-1} are observed, associated with the aliphatic C − H stretching and deforming vibrations. However, the peak intensity exhibited reduction with the increased temperature from 300 to 400 °C, which indicated that the decomposition of C—H alkyl groups is favourable at high temperatures. Interestingly, the absorbance peak around 1700 cm^{-1}, which is attributed to C═O, was absent in the FTIR spectra of hydrochar. It could be due to the deformation of C═O of the organic substances of feedstock during the SbWG process [49]. Meanwhile, the bands observed at 1436–1477 cm^{-1} correspond to the aliphatic C—H bending, which could be linked to the C—H vibration [50]. The strong peaks observed at 995–1009 cm^{-1} are associated with the stretching vibrations from the aromatic C—H group, confirming that hydrochar contains aromatic compounds. Furthermore, the weak bands at 593–806 cm^{-1} appeared, closely linked to the existence of polycyclic aromatic hydrocarbons (PAHs), as reported in the previous study [51].

The FTIR spectra of hydrochar produced from the SbWG reaction of 5 wt% feedstock concentration (see Fig. 6b) are almost the same as at 1 wt%. The significant difference is only observed at the broadband at 1008 to 1261 cm^{-1}, which was split into several bands. It could be due to the deformation of the C—O bonds of polysaccharides and aromatic chars, as reported by Liu et al. [52]. Increasing temperature weakened the band at 1008 cm^{-1}, probably due to the degradation of organic materials such as a polysaccharide. Overall, the FTIR spectra of hydrochar from the SbWG of *U. lactuca* show the existence of aromatic compounds. The FTIR spectra correspond to the result of ultimate analysis confirming the high carbon content in hydrochar.

3.3.3. Surface morphology

The surface morphology of macroalgal feedstock and its hydrochar was compared using SEM to observe the morphological changes during the SbWG process. A comparison of the SEM photographs for *U. lactuca* and its hydrochar at different temperatures is presented in Fig. 7. It should be noted that the reaction time of 60 min was selected in this study to compare the morphological structure of macroalgal feedstock and its hydrochar.

As clearly shown in this figure, the morphology of macroalgal feedstock exhibited different characteristics from its hydrochar. The SbWG process could deform the surface of macroalgal feedstock even with some cracks, resulting in a smaller size of hydrochar than the macroalga feedstock. Furthermore, some voids were also observed in macro-pores of hdyrochar, which could be attributed to more volatiles released during subcritical water gasification. Nevertheless, increasing the temperature from 300 to 400 °C could not significantly affect the pore size of hydrochar. More voids that appeared in hydrochar than the biomass feedstock have been reported in the previous studies [34,53,54]. Hence, the exploration of hydrochar-derived macroalgae as renewable porous carbon-based materials for the application of catalyst, adsorbent, or even energy storage must be intriguing to be done in the future.

3.4. Kinetic modeling of macroalgal degradation

The kinetics model of macroalgal degradation during the SbWG process was determined to quantify the effect of temperature on product distribution. The model was assumed following Arun et al. [36]

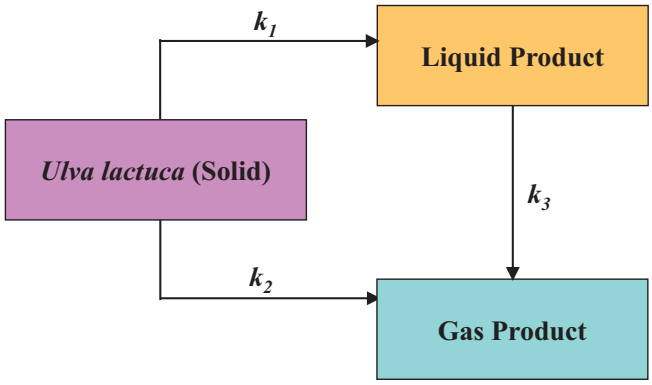

Fig. 8. Reaction pathways of macroalgal decomposition during sub-critical water gasification.

explanation, that a high concentration of feedstock results in incomplete degradation. Furthermore, the kinetic model was determined based on the solid, liquid, and gas yields, adapted from the previous study of Mainil and Matsumura [55], who determined the kinetics during SCWG of palm oil mills effluent (POME). The reaction pathways of macroalgal decomposition during SbWG are shown in Fig. 8. The *U. lactuca* feedstock (solid) was decomposed into the liquid (k_1), whereas some solid macroalgae were converted to the gaseous product (k_2). In the meantime, the liquid product was also changed to produce gas (k_3).

Based on the reaction pathways above, the rate of change in product yield can be expressed as follows:

$$dY(solid)/dt = -(k_1 + k_2)Y(solid) \quad (5)$$

$$dY(liquid)/dt = k_1 Y(solid) - k_3 Y(liquid) \quad (6)$$

$$dY(gas)/dt = k_2 Y(solid) + k_3\ Y(liquid) \quad (7)$$

where t denotes reaction time [s], k is reaction rate constant [s^{-1}], and $Y(X)$ represents the yield of product X [−].

Using the same technique with the previous studies [37,38,56], the least-squares-error (LSE) method was employed to determine the reaction rate constants. The results of the fitting curve for feedstock concentration of 1 wt% are shown in Fig. 9 (a)–(c). Meanwhile, the fitting curve for feedstock concentration of 5 wt% is presented in Fig. S2. As depicted by the parity plot (see Fig. 9 (d)), the high r^2 (coefficient of determination) value was achieved, confirming that the model can reproduce the trends of most product yields.

The reaction rate constants obtained for the reaction pathways of *U. lactuca* decomposition at operating temperatures (300–400 °C) are shown in Table S3. The correlation of the temperature on the rate constants was determined by the Arrhenius equation (Eq. (8)) to calculate the activation energy and pre-exponential factor.

$$k = Ae^{(-Ea/RT)} \quad (8)$$

where T represents reaction temperature [K], Ea represents activation energy [kJ mol^{-1}], R represents the reaction rate constant of universal gas [8.314 J mol^{-1} K^{-1}], and A represents the pre-exponential factor [s^{-1}].

Fig. 10 shows the Arrhenius plots for the SbWG of *U. lactuca*. Expectedly, the straight line between the logarithm of reaction rate constant (ln k) and the inverse temperatures (1/T) was observed, confirming that rate constants for the product resulting from SbWG of *U. lactuca* follow the Arrhenius equation. The activation energies and pre-exponential factors determined for the SbWG of *U. lactuca* are

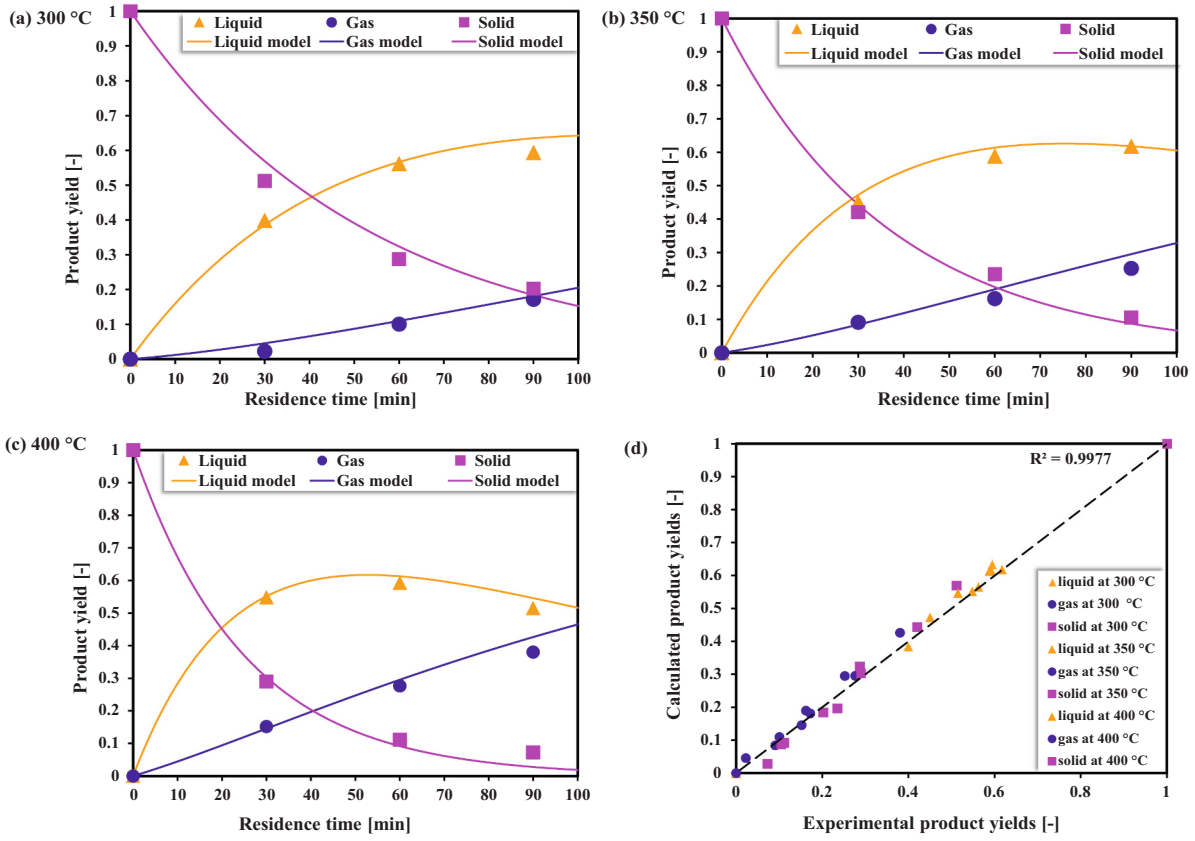

Fig. 9. Product distribution from experiment (symbol) and kinetic model (line) at feedstock concentration of 1 wt% and temperature of (a) 300 °C; (b) 350 °C; (c) 400 °C; and (d) parity plot.

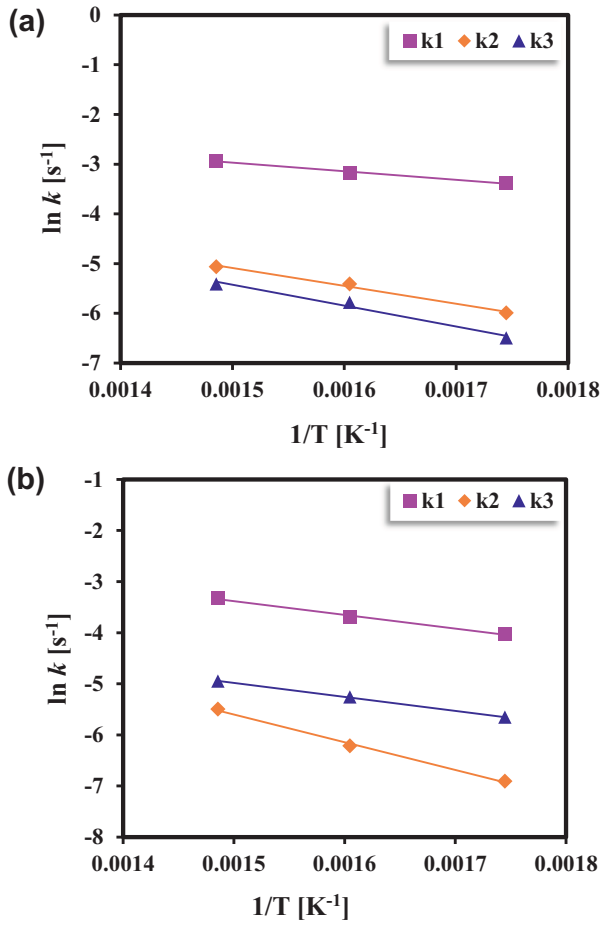

Fig. 10. Arrhenius plot of subcritical water gasification of *Ulva* sp. at feedstock concentration of (a) 1 wt% and (b) 5 wt% (Exp. Conditions: 300–400 °C).

Table 2
Activation energies (*Ea*) and pre-exponential factors (*A*) obtained for SbWG of *U. lactuca* (Experimental conditions: 300–400 °C and feedstock concentration of 1 and 5 wt%).

Kinetic parameters	Feedstock concentration of 1 wt %		Feedstock concentration of 5 wt %	
	Activation energy, E_a [kJ mol^{-1}]	Pre-exponential factor, A [s^{-1}]	Activation energy, E_a [kJ mol^{-1}]	Pre-exponential factor, A [s^{-1}]
k_1	14.36	1.14×10^{-2}	22.27	3.14×10^{-2}
k_2	29.93	2.28×10^{-2}	45.14	2.12×10^{-1}
k_3	34.98	4.04×10^{-2}	23.79	4.43×10^{-2}

presented in Table 2. Overall, the activation energies for SbWG of *U. lactuca* at feedstock concentration of 5 wt% was higher than that at 1 wt%. It indicates that high energy is needed to decompose the solid macroalgae at high concentration instead of low concentration. At a feedstock concentration of 1 wt%, the activation energies were calculated between 14.36 and 34.98 kJ. Pre-exponential factors to convert solid to liquid, solid to gas, and liquid to gas products were found to be 1.14×10^{-2}, 2.28×10^{-3}, and 4.04×10^{-2} s^{-1}, respectively. Meanwhile, the reaction with 5 wt% of macroalgal feedstock had activation energies between 22.27 and 45.14 kJ mol^{-1} with the pre-exponential factors of 3.14×10^{-2}, 2.12×10^{-1}, and 4.43×10^{-2} s^{-1} for the conversion of solid to liquid, solid to gas, and liquid to gas products, respectively.

Furthermore, it is worth noting that at low feedstock concentration, the highest activation energy was found to convert liquid to gas (k_3). In contrast, at high feedstock concentration, the highest value was observed to convert solid to gas (k_2). It could be attributed to the fact that the macromolecule in biomass (carbohydrate, protein, etc.) at low feedstock concentration was possibly diluted into the liquid phase. It is further decomposed into non-condensable gaseous products.

4. Conclusion

In this work, simultaneous production of green fuels (syngas and hydrochar) from green algae *U. lactuca* was performed using non-catalytic SbWG. The results revealed that the yield of the gaseous product increased while hydrochar yield decreased with high temperature (300–400 °C) and long reaction time (30–90 min). The highest H_2 content was achieved at 400 °C, 90 min, and feedstock concentration of 1 wt%. The SbWG process significantly decreased the macroalgal feedstock's O/C and H/C atomic ratios from 0.82 and 1.90 to 0.37–0.68 and 0.63–1.25, respectively. It confirms that dehydration and decarboxylation reactions have occurred throughout the SbWG process. The heating values of macroalgal hydrochar increased with temperature and time, with the highest HHVs of 22.93 MJ kg^{-1} comparable to the low-ranked coals. Based on the SEM analysis, the SbWG process could deform the surface of macroalgal feedstock, generating a higher surface area in hydrochar. The kinetic model of SbWG of *U. lactuca* was determined the activation energies to be around 14.36 to 34.98 kJ mol^{-1} and 22.27 to 45.14 kJ mol^{-1} for feedstock concentrations of 1 and 5 wt%, respectively. Overall, the finding highlights that the simultaneous production of syngas and hydrochar could be attained by SbWG of macroalgae. However, the optimization to increase H_2 yield and process evaluation needs to be conducted in the future.

CRediT authorship contribution statement

Obie Farobie: Conceptualization, Methodology, Writing – original draft, Resources, Formal analysis, Data curation, Project administration, Funding acquisition. **Novi Syaftika:** Writing – review & editing, Investigation, Resources. **Imron Masfuri:** Investigation, Data curation. **Tyas Puspita Rini:** Investigation, Formal analysis. **Dovan P.A. Lanank Es:** Investigation, Formal analysis. **Asep Bayu:** Investigation, Resources. **Apip Amrullah:** Methodology, Formal analysis. **Edy Hartulistiyoso:** Writing – review & editing, Supervision. **Navid R. Moheimani:** Writing – review & editing, Conceptualization. **Surachai Karnjanakom:** Writing – review & editing. **Yukihiko Matsumura:** Writing – review & editing, Supervision.

Declaration of competing interest

The authors declare that they have no known competing financial interests or personal relationships that could have appeared to influence the work reported in this paper.

Data availability

Data will be made available on request.

Acknowledgments

The authors wish to thank the Indonesian Endowment Fund for Education (LPDP) and the Indonesian Science Fund (DIPI) for generous financial support through the International Research Collaboration–RISPRO Funding Program “RISPRO KI” (Grant Number RISPRO/KI/B1/KOM/12/11684/1/2020). We are also grateful to the National Research and Innovation Agency (BRIN), Indonesia, for the provision of analytical instruments (FTIR, CHNS analyzer, and SEM) to support this research.

Appendix A. Supplementary data

Supplementary data to this article can be found online at https://doi.org/10.1016/j.algal.2022.102834.

References

[1] J.Q. Bond, A.A. Upadhye, H. Olcay, G.A. Tompsett, J. Jae, R. Xing, D.M. Alonso, D. Wang, T. Zhang, R. Kumar, A. Foster, S.M. Sen, C.T. Maravelias, R. Malina, S.R. H. Barrett, R. Lobo, C.E. Wyman, J.A. Dumesic, G.W. Huber, Production of renewable jet fuel range alkanes and commodity chemicals from integrated catalytic processing of biomass, Energy Environ. Sci. 7 (2014) 1500–1523, https://doi.org/10.1039/c3ee43846e.

[2] O. Farobie, Y. Matsumura, Energy analysis for the production of biodiesel in a spiral reactor using supercritical tert-butyl methyl ether (MTBE), Bioresour. Technol. 196 (2015) 65–71, https://doi.org/10.1016/j.biortech.2015.07.049.

[3] A.C. Fernandes, B. Biswas, J. Kumar, T. Bhaskar, U.D. Muraleedharan, Valorization of the red macroalga Gracilaria corticata by hydrothermal liquefaction: product yield improvement by optimization of process parameters, Bioresour. Technol. Rep. 15 (2021), 100796, https://doi.org/10.1016/j.biteb.2021.100796.

[4] J.S. Yuan, X. Wang, C.N. Stewart, Biomass feedstock: diversity as a solution, Biofuels 2 (2011) 491–493, https://doi.org/10.4155/bfs.11.135.

[5] J.J. Milledge, B. Smith, P.W. Dyer, P. Harvey, Macroalgae-derived biofuel: a review of methods of energy extraction from seaweed biomass, Energies 7 (2014) 7194–7222, https://doi.org/10.3390/en7117194.

[6] O. Farobie, Y. Matsumura, N. Syaftika, A. Amrullah, E. Hartulistiyoso, A. Bayu, N. R. Moheimani, S. Karnjanakom, G. Saefurahman, Recent advancement on hydrogen production from macroalgae via supercritical water gasification, Bioresour. Technol. Rep. 16 (2021), 100844, https://doi.org/10.1016/j.biteb.2021.100844.

[7] S. Deshmukh, R. Kumar, K. Bala, Microalgae biodiesel: a review on oil extraction, fatty acid composition, properties and effect on engine performance and emissions, Fuel Process. Technol. 191 (2019) 232–247, https://doi.org/10.1016/j.fuproc.2019.03.013.

[8] P. Biller, A.B. Ross, Biofuels hydrothermal processing of algal biomass for the production of biofuels and chemicals hydrothermal processing of algal biomass for the production of biofuels and chemicals, Biofuels 3 (2012) 603–623.

[9] V.H. Smith, Eutrophication of freshwater and coastal marine ecosystems: a global problem, Environ. Sci. Pollut. Res. 10 (2003) 126–139, https://doi.org/10.1065/espr2002.12.142.

[10] A. Shrestha, B. Acharya, A.A. Farooque, Study of hydrochar and process water from hydrothermal carbonization of sea lettuce, Renew. Energy 163 (2021) 589–598, https://doi.org/10.1016/j.renene.2020.08.133.

[11] S. Rinehart, M. Guidone, A. Ziegler, T. Schollmeier, C. Thornber, Overwintering strategies of bloom-forming ulva species in Narragansett Bay, Rhode Island, USA, Bot. Mar. 57 (2014) 337–341, https://doi.org/10.1515/bot-2013-0122.

[12] L.R.D. Human, J.B. Adams, B.R. Allanson, Insights into the cause of an Ulva lactuca Linnaeus bloom in the Knysna Estuary, S.Afr.J. Bot. 107 (2016) 55–62, https://doi.org/10.1016/j.sajb.2016.05.016.

[13] J.J. Milledge, P.J. Harvey, Golden tides: problem or golden opportunity? The valorisation of Sargassum from beach inundations, J. Mar. Sci. Eng. 4 (2016), https://doi.org/10.3390/jmse4030060.

[14] J. Gichuki, R. Omondi, P. Boera, T. Okorut, A.S. Matano, T. Jembe, A. Ofulla, Water hyacinth Eichhornia crassipes (Mart.) Solms-Laubach dynamics and succession in the Nyanza Gulf of Lake Victoria (East Africa): implications for water quality and biodiversity conservation, Sci. World J. 2012 (2012), https://doi.org/10.1100/2012/106429.

[15] Y.K. Leong, W.H. Chen, D.J. Lee, J.S. Chang, Supercritical water gasification (SCWG) as a potential tool for the valorization of phycoremediation-derived waste algal biomass for biofuel generation, J. Hazard. Mater. 418 (2021), 126278, https://doi.org/10.1016/j.jhazmat.2021.126278.

[16] Y. Hu, L. Qi, K. Tirumala Venkateswara Rao, B. Zhao, H. Li, Y. Zeng, C. (Charles) Xu, Supercritical water gasification of biocrude oil from low-temperature liquefaction of algal lipid extraction residue, Fuel 276 (2020), 118017, https://doi.org/10.1016/j.fuel.2020.118017.

[17] S.H. Ho, C. Zhang, F. Tao, C. Zhang, W.H. Chen, Microalgal torrefaction for solid biofuel production, Trends Biotechnol. 38 (2020) 1023–1033, https://doi.org/10.1016/j.tibtech.2020.02.009.

[18] A. Amrullah, O. Farobie, R. Widyanto, Pyrolysis of purun tikus (Eleocharis dulcis): product distributions and reaction kinetics, Bioresour. Technol. Rep. 13 (2021), 100642, https://doi.org/10.1016/j.biteb.2021.100642.

[19] T. Samanmulya, O. Farobie, Y. Matsumura, Gasification characteristics of aminobutyric acid and serine as model compounds of proteins under supercritical water conditions, J. Japan Pet. Inst. 60 (2017) 34–40, https://doi.org/10.1627/jpi.60.34.

[20] P.G. Duan, S.C. Li, J.L. Jiao, F. Wang, Y.P. Xu, Supercritical water gasification of microalgae over a two-component catalyst mixture, Sci. Total Environ. 630 (2018) 243–253, https://doi.org/10.1016/j.scitotenv.2018.02.226.

[21] L. Yan, Y. Wang, J. Li, Y. Zhang, L. Ma, F. Fu, B. Chen, H. Liu, Hydrothermal liquefaction of Ulva prolifera macroalgae and the influence of base catalysts on products, Bioresour. Technol. 292 (2019), 121286, https://doi.org/10.1016/j.biortech.2019.03.125.

[22] J. Xu, X. Dong, Y. Wang, Hydrothermal liquefaction of macroalgae over various solids, basic or acidic oxides and metal salt catalyst: products distribution and characterization, Ind. Crop. Prod. 151 (2020), 112458, https://doi.org/10.1016/j.indcrop.2020.112458.

[23] C. Ma, J. Geng, D. Zhang, X. Ning, Hydrothermal liquefaction of macroalgae: influence of zeolites based catalyst on products, J. Energy Inst. 93 (2020) 581–590, https://doi.org/10.1016/j.joei.2019.06.007.

[24] E. Steinbruch, D. Drabik, M. Epstein, S. Ghosh, M.S. Prabhu, M. Gozin, A. Kribus, A. Golberg, Hydrothermal processing of a green seaweed Ulva sp. for the production of monosaccharides, polyhydroxyalkanoates, and hydrochar, Bioresour. Technol. 318 (2020), 124263, https://doi.org/10.1016/j.biortech.2020.124263.

[25] D. Lachos-Perez, A.B. Brown, A. Mudhoo, J. Martinez, M.T. Timko, M.A. Rostagno, T. Forster-Carneiro, Applications of subcritical and supercritical water conditions for extraction, hydrolysis, gasification, and carbonization of biomass: a critical review, Biofuel Res. J. 4 (2017) 611–626, https://doi.org/10.18331/BRJ2017.4.2.6.

[26] H. Su, D. Hantoko, M. Yan, Y. Cai, E. Kanchanatip, J. Liu, X. Zhou, S. Zhang, Evaluation of catalytic subcritical water gasification of food waste for hydrogen production: effect of process conditions and different types of catalyst loading, Int. J. Hydrog. Energy 44 (2019) 21451–21463, https://doi.org/10.1016/j.ijhydene.2019.06.203.

[27] J. Sun, L. Xu, G.hua Dong, S. Nanda, H. Li, Z. Fang, J.A. Kozinski, A.K. Dalai, Subcritical water gasification of lignocellulosic wastes for hydrogen production with Co modified Ni/Al2O3 catalysts, J. Supercrit. Fluids 162 (2020) 2–11, https://doi.org/10.1016/j.supflu.2020.104863.

[28] A.E. Brown, G.L. Finnerty, M.A. Camargo-Valero, A.B. Ross, Valorisation of macroalgae via the integration of hydrothermal carbonisation and anaerobic digestion, Bioresour. Technol. 312 (2020), 123539, https://doi.org/10.1016/j.biortech.2020.123539.

[29] K.P.R. Dandamudi, K. Muhammed Luboowa, M. Laideson, T. Murdock, M. Seger, J. McGowen, P.J. Lammers, S. Deng, Hydrothermal liquefaction of Cyanidioschyzon merolae and Salicornia bigelovii Torr.: the interaction effect on product distribution and chemistry, Fuel 277 (2020), 118146, https://doi.org/10.1016/j.fuel.2020.118146.

[30] R.B. Carpio, Y. Zhang, C.T. Kuo, W.T. Chen, L.C. Schideman, R. de Leon, Effects of reaction temperature and reaction time on the hydrothermal liquefaction of demineralized wastewater algal biomass, Bioresour. Technol. Rep. 14 (2021), 100679, https://doi.org/10.1016/j.biteb.2021.100679.

[31] C.G. Khoo, M.K. Lam, A.R. Mohamed, K.T. Lee, Hydrochar production from high-ash low-lipid microalgal biomass via hydrothermal carbonization: effects of operational parameters and products characterization, Environ. Res. 188 (2020), 109828, https://doi.org/10.1016/j.envres.2020.109828.

[32] S. Nizamuddin, H.A. Baloch, G.J. Griffin, N.M. Mubarak, A.W. Bhutto, R. Abro, S. A. Mazari, B.S. Ali, An overview of effect of process parameters on hydrothermal carbonization of biomass, Renew. Sustain. Energy Rev. 73 (2017) 1289–1299, https://doi.org/10.1016/j.rser.2016.12.122.

[33] M. Kaewpanha, G. Guan, X. Hao, Z. Wang, Y. Kasai, K. Kusakabe, A. Abudula, Steam co-gasification of brown seaweed and land-based biomass, Fuel Process. Technol. 120 (2014) 106–112, https://doi.org/10.1016/j.fuproc.2013.12.013.

[34] Y. Su, L. Liu, D. Xu, H. Du, Y. Xie, Y. Xiong, S. Zhang, Syngas production at low temperature via the combination of hydrothermal pretreatment and activated carbon catalyst along with value-added utilization of tar and bio-char, Energy Convers. Manag. 205 (2020), 112382, https://doi.org/10.1016/j.enconman.2019.112382.

[35] J. Wu, Z. Hu, Z. Miao, W. Wu, E. Jiang, Effect of alkaline earth metal ca in rice husk during chemical looping gasification process, Fuel 299 (2021), 120902, https://doi.org/10.1016/j.fuel.2021.120902.

[36] J. Arun, K.P. Gopinath, P.S. SundarRajan, R. Malolan, S. Adithya, R. Sai Jayaraman, P. Srinivaasan Ajay, Hydrothermal liquefaction of Scenedesmus obliquus using a novel catalyst derived from clam shells: solid residue as catalyst for hydrogen production, Bioresour. Technol. 310 (2020), 123443, https://doi.org/10.1016/j.biortech.2020.123443.

[37] A. Amrullah, Y. Matsumura, Supercritical water gasification of sewage sludge in continuous reactor, Bioresour. Technol. 249 (2018) 276–283, https://doi.org/10.1016/j.biortech.2017.10.002.

[38] P.R. Nurcahyani, S. Hashimoto, Y. Matsumura, Supercritical water gasification of microalgae with and without oil extraction, J. Supercrit. Fluids 165 (2020), 104936, https://doi.org/10.1016/j.supflu.2020.104936.

[39] O. Farobie, P. Changkiendee, S. Inoue, T. Inoue, Y. Kawai, T. Noguchi, H. Tanigawa, Y. Matsumura, Effect of the heating rate on the supercritical water gasification of a glucose/guaiacol mixture, Ind. Eng. Chem. Res. 56 (2017) 6401–6407, https://doi.org/10.1021/acs.iecr.7b00640.

[40] N.Y. Acelas, D.P. López, D.W.F. Wim Brilman, S.R.A. Kersten, A.M.J. Kootstra, Supercritical water gasification of sewage sludge: gas production and phosphorus recovery, Bioresour. Technol. 174 (2014) 167–175, https://doi.org/10.1016/j.biortech.2014.10.003.

[41] J. Chen, S. Li, Characterization of biofuel production from hydrothermal treatment of hyperaccumulator waste (Pteris vittata L.) in sub- and supercritical water, RSC Adv. 10 (2020) 2160–2169, https://doi.org/10.1039/c9ra09410e.

[42] E.M. Moghaddam, A. Goel, M. Siedlecki, K. Michalska, O. Yakaboylu, W. de Jong, Supercritical water gasification of wet biomass residues from farming and food production practices: lab-scale experiments and comparison of different modelling approaches, Sustain.Energy Fuel 5 (2021) 1521–1537, https://doi.org/10.1039/d0se01635g.

[43] D. Selvi Gökkaya, M. Sert, M. Sağlam, M. Yüksel, L. Ballice, Hydrothermal gasification of the isolated hemicellulose and sawdust of the white poplar (Populus

alba L.), J. Supercrit. Fluids 162 (2020), https://doi.org/10.1016/j.supflu.2020.104846.
[44] Y. Graz, S. Bostyn, T. Richard, P.E. Bocanegra, E. De Bilbao, J. Poirier, I. Gokalp, Hydrothermal conversion of Ulva macro algae in supercritical water, J. Supercrit. Fluids 107 (2016) 182–188, https://doi.org/10.1016/j.supflu.2015.07.038.
[45] O. Norouzi, F. Safari, S. Jafarian, A. Tavasoli, A. Karimi, Hydrothermal gasification performance of Enteromorpha intestinalis as an algal biomass for hydrogen-rich gas production using Ru promoted Fe–Ni/Γ-Al2O3 nanocatalysts, Energy Convers. Manag. 141 (2017) 63–71, https://doi.org/10.1016/j.enconman.2016.04.083.
[46] L. Azaare, M.K. Commeh, A.M. Smith, F. Kemausuor, Co-hydrothermal carbonization of pineapple and watermelon peels: effects of process parameters on hydrochar yield and energy content, Bioresour. Technol. Rep. 15 (2021), 100720, https://doi.org/10.1016/j.biteb.2021.100720.
[47] Z. Luo, W. Tao, CFBC And BFBC of Low-rank Coals, Elsevier Ltd, 2017, https://doi.org/10.1016/B978-0-08-100895-9.00007-3.
[48] G. Gascó, J. Paz-Ferreiro, M.L. Álvarez, A. Saa, A. Méndez, Biochars and hydrochars prepared by pyrolysis and hydrothermal carbonisation of pig manure, Waste Manag. 79 (2018) 395–403, https://doi.org/10.1016/j.wasman.2018.08.015.
[49] N. Qadi, K. Takeno, A. Mosqueda, M. Kobayashi, Y. Motoyama, K. Yoshikawa, Effect of hydrothermal carbonization conditions on the physicochemical properties and gasification reactivity of energy grass, EnergyFuels 33 (2019) 6436–6443, https://doi.org/10.1021/acs.energyfuels.9b00994.
[50] A. Hasanoğlu, I. Demirci, A. Seçer, Hydrogen production by gasification of kenaf under subcritical liquid–vapor phase conditions, Int. J. Hydrog. Energy (2019) 14127–14136, https://doi.org/10.1016/j.ijhydene.2018.08.165.
[51] A. Iaccarino, R. Gautam, S.M. Sarathy, Bio-oil and biochar production from halophyte biomass: effects of pre-treatment and temperature on Salicornia bigelovii pyrolysis, Sustain.Energy Fuel 5 (2021) 2234–2248, https://doi.org/10.1039/d0se01664k.
[52] Z. Liu, A. Quek, S. Kent Hoekman, R. Balasubramanian, Production of solid biochar fuel from waste biomass by hydrothermal carbonization, Fuel 103 (2013) 943–949, https://doi.org/10.1016/j.fuel.2012.07.069.
[53] A.I. Osman, C. Farrell, A.H. Al-Muhtaseb, J. Harrison, D.W. Rooney, The production and application of carbon nanomaterials from high alkali silicate herbaceous biomass, Sci. Rep. 10 (2020) 1–13, https://doi.org/10.1038/s41598-020-59481-7.
[54] J.E. Omoriyekomwan, A. Tahmasebi, J. Zhang, J. Yu, Formation of hollow carbon nanofibers on bio-char during microwave pyrolysis of palm kernel shell, Energy Convers. Manag. 148 (2017) 583–592, https://doi.org/10.1016/j.enconman.2017.06.022.
[55] R.I. Mainil, Y. Matsumura, New application of supercritical water gasification to palm oil mill effluent: gasification and phosphorus recovery, EnergyFuels 33 (2019) 11145–11152, https://doi.org/10.1021/acs.energyfuels.9b02729.
[56] N. Paksung, J. Pfersich, P.J. Arauzo, D. Jung, A. Kruse, Structural effects of cellulose on hydrolysis and carbonization behavior during hydrothermal treatment, ACS Omega 5 (2020) 12210–12223, https://doi.org/10.1021/acsomega.0c00737.